

# Polymer Chemistry

Accepted Manuscript



This is an *Accepted Manuscript*, which has been through the Royal Society of Chemistry peer review process and has been accepted for publication.

*Accepted Manuscripts* are published online shortly after acceptance, before technical editing, formatting and proof reading. Using this free service, authors can make their results available to the community, in citable form, before we publish the edited article. We will replace this *Accepted Manuscript* with the edited and formatted *Advance Article* as soon as it is available.

You can find more information about *Accepted Manuscripts* in the [Information for Authors](#).

Please note that technical editing may introduce minor changes to the text and/or graphics, which may alter content. The journal's standard [Terms & Conditions](#) and the [Ethical guidelines](#) still apply. In no event shall the Royal Society of Chemistry be held responsible for any errors or omissions in this *Accepted Manuscript* or any consequences arising from the use of any information it contains.



Journal Name

ARTICLE

## A composition-controlled cross-linking resin network through rapid visible-light photo-copolymerization

Yin Yang,<sup>a</sup> Aaron Urbas,<sup>b</sup> Andres Gonzalez-Bonet,<sup>a</sup> Richard J. Sheridan,<sup>c</sup> Jonathan Seppala,<sup>c</sup> Kathryn L. Beers,<sup>c</sup> and Jirun Sun<sup>\*a</sup>

Received 00th January 20xx,  
Accepted 00th January 20xx

DOI: 10.1039/x0xx00000x

www.rsc.org/

An assembly that delivers well-defined functional materials, clinically practical procedures to make these materials *in situ*, and appropriate analytical tools for chemical structure and kinetic studies is desirable, though currently unavailable. Herein, we introduce a system that addresses this need through the development and characterization of a cross-linking resin network, which is achieved through rapid, visible-light induced polymerization in a solvent-free environment. This resin network is the result of co-polymerization of a distyrenyl-monomer with a dimethacryl-monomer. Ninety percent of vinyl conversion is achieved in seconds. In addition, an azeotropic composition is identified and confirmed through static end-point evaluation, sol-gel experiment, kinetic study, and mathematical modeling of data acquired via FTIR, real-time Raman and <sup>1</sup>H NMR spectroscopies. These results yield opportunities for the design and development of new functional materials to be used in various applications.

### Introduction

With the ever-growing impetus to build new advanced functional materials, many synthetic approaches and conceptual designs have been developed,<sup>1–8</sup> and opportunities are opened.<sup>9–13</sup> A clinically implementable system that makes high performance functional polymeric materials on site, especially those with well-defined chemical structures, is appealing for various applications, including medical devices, electronic devices, and the automobile industry.<sup>14–18</sup> Besides the demand for new polymers, any novel compositions need appropriate analytical tools to determine their chemical structures and understand polymerization kinetics.<sup>19–21</sup> The primary instruments for polymerization kinetic studies, including MALDI-ToF-MS, <sup>1</sup>H NMR and size exclusion chromatograph, are capable of assessing linear polymers, but have difficulties with cross-linked resins.<sup>22–26</sup>

Herein, we introduce an all-in-one platform through the development and characterization of a cross-linking resin network, which is prepared by rapid visible-light initiated polymerization in a solvent-free environment. Free radical polymerization initiated by visible light is extremely versatile and biocompatible.<sup>27–31</sup> It has been extensively used in

dentistry to treat tooth caries, in non-toxic packaging, and recently, in desktop 3D-printing.<sup>32–36</sup> Here, two monomers with free-radical polymerizable vinyl groups are used as models. One monomer, triethylene glycol-divinylbenzyl ether (TEG-DVBE), is lab-prepared. It is stable to hydrolysis and esterase degradation because of the ether-based chemical structure.<sup>37</sup> The other monomer, urethane dimethacrylate (UDMA), is one of the key components in making medical devices including dental restorative materials to treat carious teeth. UDMA has shown a superior toughness as a base-monomer in resins and composites compared to bis-phenol-A-glycidyl-dimethacrylate (Bis-GMA) based monomers.<sup>38–40</sup> The mixtures of TEG-DVBE/UDMA are liquids at room temperature, in which the photo-initiators, i.e. camphorquinone/amine, are soluble. Consequently, the photo-polymerization of the monomer mixtures is initiated by visible light ( $\lambda = 440 - 490$  nm) in a solvent-free environment. In addition, both TEG-DVBE and UDMA have two polymerizable vinyl groups. Therefore, they produce cross-links upon curing. The copolymers are designed to produce synergetic effects from both monomers: rapid free-radical photo-polymerization and good mechanical performance of UDMA, and the resistance to hydrolysis and esterase degradation of TEG-DVBE. Furthermore, due to the significant viscosity difference between the methacrylate-derivative monomer and the styrene-derivative monomer (UDMA  $\gg$  TEG-DVBE), this monomer combination provides a sophisticated model for studying kinetics of free radical copolymerization.

### Results and discussion

#### Validation of analytical methods

<sup>a</sup> Dr. Anthony Volpe Research Center, American Dental Association Foundation, National Institute of Standards and Technology, Gaithersburg, MD 20899, USA. E-mail: jsun@nist.gov

<sup>b</sup> Biosystems and Biomaterials Division, Materials and Measurement Laboratory, National Institute of Standards and Technology, Gaithersburg, MD 20899, USA

<sup>c</sup> Materials Science and Engineering Division, Materials and Measurement Laboratory, National Institute of Standards and Technology, Gaithersburg, MD 20899, USA

Electronic Supplementary Information (ESI) available: Original spectra for structural characterization, and additional figures. See DOI: 10.1039/x0xx00000x

FTIR spectroscopy, real-time Raman micro-spectroscopy, and  $^1\text{H}$  NMR spectroscopy were used to evaluate the composition of monomer mixtures and their copolymers. The absorbance or scattering of vinyl groups on TEG-DVBE (a styrene-derivative) and UDMA (a methacrylate-derivative) were identified, separated, and quantified using FTIR spectroscopy and Raman spectroscopy. The vinyl groups on TEG-DVBE formed a stronger conjugation with their benzene rings than the vinyl groups on UDMA did with carboxyl groups. In addition, the di-substitution (methyl and carboxyl) of the  $\beta$ -carbon of methacrylates may cause the C=C stretching to shift to a lower energy. As a result, the vinyl groups on TEG-DVBE and UDMA exhibited peaks at approximately  $1629\text{ cm}^{-1}$  and  $1638\text{ cm}^{-1}$ , respectively, in both FTIR and Raman spectra (Fig. 1A and 1B). The separation and quantification of the C=C peaks of these two monomers was realized through peak-fitting using mathematical models developed for FTIR and Raman (see SI for details, Fig. S2A and S2B). Fig. 1C shows an example of FTIR peak-fitting results of an equimolar monomer mixture. In the wavenumber ranging from  $1580\text{ cm}^{-1}$  and  $1660\text{ cm}^{-1}$ , four peaks were identified. Besides the absorption of C=C stretching of vinyl groups, the C=C stretching of the benzene ring from TEG-DVBE ( $1612\text{ cm}^{-1}$ ) and N-H bending from UDMA ( $1623\text{ cm}^{-1}$ ) were observed, respectively.<sup>41</sup>

The FTIR and Raman methods are convenient in assessing the degree of vinyl conversion (DC) and composition of TEG-DVBE and UDMA in polymers during the polymerization process.<sup>42, 43</sup> The specimen can be a liquid, solid, or gel.  $^1\text{H}$  NMR provides a more quantitative measurement of the monomer compositions, but requires that the materials be fully dissolved in deuterated solvents. In this work,  $^1\text{H}$  NMR was implemented as a complimentary method to validate results from FTIR and Raman. Fig. 1D shows the correlation between compositions calculated from Raman spectra and the corresponding mole ratios of UDMA to TEG-DVBE, determined by  $^1\text{H}$  NMR. Raman-compositions were calculated based on direct classical least

squares (CLS) fitting using the pure monomer spectra.<sup>44, 45</sup> In our experimental results, the Raman-compositions and NMR mole ratios had a high degree of correlation ( $R^2 = 0.999$ ). In the following discussion, FTIR and  $^1\text{H}$  NMR will be used to assess the end-point DCs and compositions. The real-time composition changes during polymerization will be evaluated through real-time Raman micro-spectroscopy.

### Rapid photo-copolymerization

One of the synergetic effects of the model monomers is the significant improvement of polymerization rate of the styrene-derivative, TEG-DVBE, by adding UDMA. Free radical homopolymerization of styrene is relatively slow in comparison with methacrylate, due to stabilization of free radicals through resonance with styrene's benzene ring. Without modifying the chemical structure of the monomer or inventing new initiators, copolymerization is one of the most efficient ways to accelerate polymer chain propagation. The rate of copolymerization is strongly affected by the competition of monomer reactivity ratios ( $r_1$  and  $r_2$ ), as a result, it overcomes the drawback of free-radical stabilization in homopolymerization of TEG-DVBE. Although substantial work has been done to improve the polymerization rate of styrenic monomers in vinyl ester resins (VERs),<sup>46, 47</sup> the polymerization rate and low degree of vinyl conversion are still limiting factors for VERs to be used clinically in dental adhesives and dental composites. Here, we demonstrate the viability of using model monomers in dental clinics by reaching DC above 70 % with 20 s of light irradiation. Fig. 2 shows the DCs of TEG-DVBE, UDMA, and the equimolar mixture of TEG-DVBE and UDMA immediately after light irradiation (light intensity at  $1600\text{ mW/cm}^2$ ) for 20 s, 40 s, and 60 s. The low DC indicates that camphorquinone / ethyl 4-N, N-dimethylaminobenzoate (CQ/amine) are not efficient initiators for TEG-DVBE homopolymerization. This initiator combination is very effective on UDMA homo-polymer and the copolymer: their DCs reaching approximately 90 % in 20 s. In Fig. 2B, a filled contour plot shows the DC of monomer mixtures as a function of the feed mole fraction of TEG-DVBE and light irradiation time. Setting DC = 70 % (yellow color in Fig. 2B) as a reference value considering the potential application in dental clinics, the

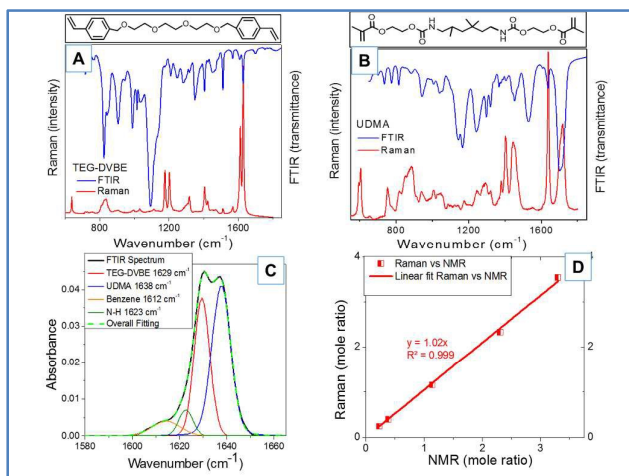


**Fig. 1** Evaluation of TEG-DVBE and UDMA using FTIR and Raman spectroscopy. (A and B) Chemical structures of TEG-DVBE and UDMA with their FTIR and Raman spectra. (C) FTIR peak fitting of an equimolar TEG-DVBE/UDMA monomer mixture; the vinyl stretching peaks of TEG-DVBE and UDMA. (D) Comparison of the compositions of monomer mixtures determined by Raman with the mole ratios determined by NMR.

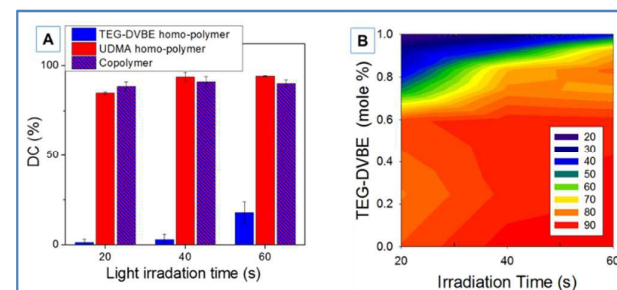


**Fig. 2** Synergetic effects on improving polymerization rate of TEG-DVBE by adding UDMA. (A) Degree of vinyl conversion (DC) of TEG-DVBE and UDMA homo-polymers and their equimolar copolymer immediately after three light ( $\lambda = 440 - 490\text{ nm}$ ; intensity =  $1600\text{ mW/cm}^2$ ) irradiation time. (B) A filled contour plot of DC of copolymers at X (light irradiation time) and Y (mole fraction of TEG-DVBE in feed monomers). The DC values are color coded (inset). From blue color to red color indicates DC values from low to high.

monomer mixtures reached this DC in 60 s when they contained 91 mole % or less of TEG-DVBE. Adding UDMA accelerated the polymerization. In only 20 s of light irradiation, the monomer mixtures containing 70 mole % or less of the styrene-derivative had a vinyl conversion over 70 %.

#### An azeotropic composition confirmed by sol-gel experiment

Another noteworthy feature is the azeotropic composition at equimolar TEG-DVBE and UDMA when CQ/amine are used as initiators. Azeotropic compositions in copolymers mean that the mole fractions of the feed monomers are retained in the polymer and are constant throughout the polymerization process.<sup>48, 49</sup>

FTIR also revealed that the DC of TEG-DVBE and UDMA in the above equimolar copolymers was the same, approximately 90%. The composition of copolymers was further evaluated by the sol-gel experiment.<sup>50</sup> To extract enough leachable materials, the light intensity was reduced to 43 mW/cm<sup>2</sup>, and low DC copolymers were obtained. **Table 1** shows the TEG-DVBE/UDMA composition in gels and solutions at three DCs. The progress of photo-polymerization was controlled by varying the time of light irradiation. Based on the peak-area analysis of the absorbance of C=C stretching in FTIR spectra and integration of <sup>1</sup>H NMR signals associated with protons on C=C, the styrene-vinyl groups and methacrylate-vinyl groups had the same mole fraction in both gels and soluble. This suggests that the equimolar composition of the feed monomers was kept in these three polymerization stages from DC = 5 % to DC = 62 %.

#### The azeotropic composition confirmed by real-time Raman spectroscopy

Real-time Raman micro-spectroscopy further confirmed that the equimolar composition was constant over time during photo-polymerization and was independent of the polymerization rate, which was controlled through light intensity and irradiation time. To achieve a step-wise polymerization, specimens were exposed to light at 4 mW/cm<sup>2</sup> for 5 s up to a total of four exposures. The multivariate CLS method standardized using pure monomer spectra was used to estimate unpolymerized monomer composition in the samples using the C=C stretching bands of TEG-DVBE and UDMA. CLS scores for each specimen were normalized to 100 for the pre-polymerized monomer mixtures. As the vinyl groups converted to polymers, the associated C=C band

**Table 1.** Composition evaluation of copolymers of equimolar TEG-DVBE/UDMA with CQ/amine by sol-gel experiment (N=3).

intensity decreased, and the DC increased accordingly. At each

Irradiation Time (s)	Overall DC (%) <sup>a</sup>	Gel fraction		Soluble fraction
		DC (%) <sup>a</sup>	TEG-DVBE/UDMA <sup>a</sup>	TEG-DVBE/UDMA <sup>b</sup>
10	5.2 ± 1.5	65 ± 1.0	1.0 ± 0.0	1.0 ± 0.0
20	32.5 ± 7.0	68 ± 1.0	1.0 ± 0.1	1.0 ± 0.0

Notes: <sup>a</sup> the values were determined by FTIR spectroscopy; <sup>b</sup> the values were determined by <sup>1</sup>H NMR spectroscopy.

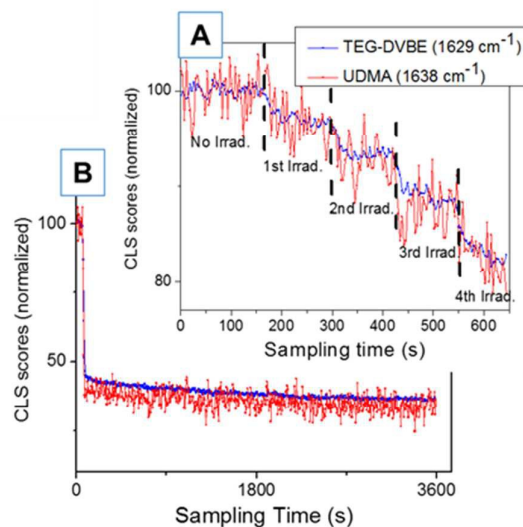


**Fig. 3** Azeotropic composition of TEG-DVBE/UDMA evaluated by real-time Raman micro-spectroscopy. (A) CLS intensity changes during a slow photo-polymerization. The specimen was irradiated by a visible light at an intensity of 4 mW/cm<sup>2</sup> for 5s. Four light irradiations were applied during the 10 min experiment. The starting time points are marked by dash lines. (B) CLS intensity changes during a fast photo-polymerization. The specimen was irradiated by a visible light at an intensity of 150 mW/cm<sup>2</sup> for 20 s. The decrease of normalized CLS scores indicates the trend of DC increase.

light irradiation (labeled by black dash lines in **Fig. 3A**), the intensity dropped immediately, which was followed by further decrease at a much slower rate, until the next irradiation. During the full time range (10 min) of this set of experiments, DC reached approximately 20 %, and the ratio of TEG-DVBE/UDMA remained 1/1. A faster photo-polymerization took place when the sample was irradiated at 150 mW/cm<sup>2</sup> for 20 s. The Raman spectra data set for this run is shown in (**Fig. S2C** and **S2D**). The normalized CLS scores as a function of sampling time are shown in **Fig. 3B**. The DC of this specimen achieved approximately 55 % immediately after light irradiation; after 1 h, the DC was approximately 65%; after 1 d, it was approximately 72 % (**Fig. S3**). During the course of this set of experiments, the ratio of TEG-DVBE and UDMA was always 1/1.

#### The azeotropic composition predicted by monomer reactivity ratios

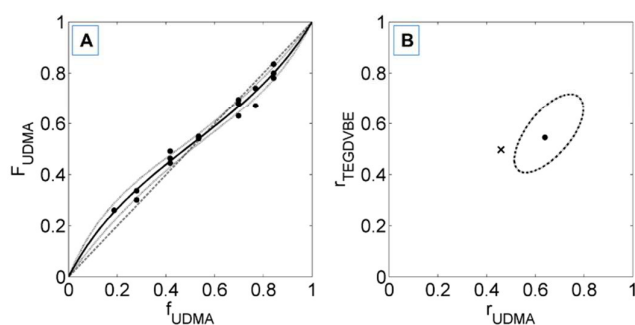
Furthermore, monomer reactivity ratios were evaluated to understand the kinetics behind the azeotropic composition at equimolar composition. The polymer composition (F) was determined by Raman micro-spectroscopy according to the CLS score ratios of TEG-DVBE and UDMA at low DCs (1 - 3 %). A classic instantaneous copolymerization equation<sup>51</sup> for non-cross-linking polymers is used to compare F with the monomer feed composition (f, mole fraction) based on an assumption that at such low DC, the two vinyl groups in one molecule act independently without interfering with each other.

$$F_1 = \frac{r_1 f_1^2 + f_1(1-f_1)}{r_1 f_1^2 + 2f_1(1-f_1) + 2r_2(1-f_1)^2}$$

The Mayo-Lewis plot is shown in **Fig. 4A**. The feed ratios of monomers do not always determine the compositions of the final material. Feeds with a molar ratio UDMA/TEG-DVBE > 0.5 are expected to produce networks depleted in their UDMA content relative to the feeds, and UDMA/TEG-DVBE < 0.5 produce networks enriched in UDMA. The composition data were fit to the above equation with a nonlinear least-squares (NLLS) optimization after van Herk.<sup>19, 22, 52-54</sup> **Fig. 4B** shows the reactivity ratios estimated by the NLLS fit bound by 95 % joint confidence intervals. The monomer reactivity ratios,  $r_{\text{UDMA}}$  and  $r_{\text{TEGDVBE}}$ , are  $0.64 \pm 0.11$  and  $0.55 \pm 0.12$ , respectively. They are slightly, but statistically significantly, higher than the reactivity ratios of styrene and methyl methacrylate,  $r_1 \approx r_2 \approx 0.5$ .<sup>19, 54</sup> These reactivity ratios suggest a polymerization mechanism somewhat biased towards cross-propagation and alternating sequences, characteristic of styrenic-methacrylic copolymer systems.

#### The effects of viscosity and monomer chemistry on composition control

Both of the sol-gel experiments and kinetic studies suggest the copolymerization of TEG-DVBE and UDMA is a monomer-chemistry-controlled process. The viscosity of monomer shows no consequential role during the polymer chain propagation, considering that the viscosity of UDMA ( $6.631 \pm 0.100$  Pa-s) is approximately 240 time higher than that of TEG-DVBE ( $0.029 \pm 0.001$  Pa-s). In contrast, copolymerization of UDMA and triethylene glycol dimethacrylate (viscosity =  $0.050$  Pa-s)<sup>50</sup> showed significantly composition drift when DC was above 20 % because the low viscosity monomers diffused faster in resin networks than the base monomers and reached the propagating chain quicker, thus more of them were converted into polymers at high DCs.<sup>50</sup> Composition shift was also common in vinyl ester resins (VERs) due to diffusion limitation



in cross-linked resin network.<sup>55</sup> Furthermore, the use of multi-styrene monomers in VERs enhanced diffusion limitation. Consequently, in addition to composition shift, low

**Fig. 4** (A) A Mayo-Lewis plot for TEG-DVBE/UDMA copolymers initiated by CQ/amine. The compositions were determined by Raman micro-spectroscopy. The black solid line corresponds to the nonlinear least-squares (NLLS) fit. The gray dotted lines indicate estimated values bound by 95 % confidence to the NLLS fit. The diagonal dashed line shows the ideal case of random polymerization. (B) Monomer reactivity ratios estimated by the NLLS fit (point) bound by 95 % joint confidence intervals (dashed ellipse). The measured reactivity ratios,  $r_{\text{UDMA}}$  and  $r_{\text{TEGDVBE}}$ , are  $0.64 \pm 0.11$  and  $0.55 \pm 0.12$ , respectively. This can be compared to typical styrene/methacrylate reactivity ratios (cross).<sup>19</sup>

polymerization rate and DC were also expected.<sup>46</sup> Apparently, all of the experiment results above demonstrated that our model monomers copolymerized in a different way from dimethacrylate copolymers and VERs.

Although the exact mechanism that leads to such rapid photo-polymerization and well-controlled azeotropic composition is yet to be defined, UDMA has dual roles: monomer and co-initiator when initiated by CQ/amine. The carbamate functional group in UDMA may form a free radical on a methylene group adjacent to its N-H groups. This may be achieved via electron transfer from the light-excited CQ. Experimentally, the photo-polymerization rate of UDMA initiated by CQ alone was similar to that by CQ/amine, and the photo-bleaching rate of CQ in UDMA also showed minimal differences with/without amine.<sup>56-59</sup>

## Experimental

### Chemicals and reagents

The commercial monomer UDMA was supplied by Esstech (Essington, PA, USA) and was used as received. TEG-DVBE was synthesized and fully characterized in house according to a previously reported procedure.<sup>37</sup> The resin formations used for this study were activated by 0.2 wt % of camphorquinone (CQ, Aldrich, Saint Louis, MO, USA) and 0.8 wt % of ethyl 4-N,N-dimethylaminobenzoate (amine, Aldrich, Saint Louis, MO, USA) for visible light photo-polymerization.

### Photo-polymerization methods

The monomer mixtures were sandwiched between two Mylar films (10  $\mu\text{L}$ , for FTIR-ATR measurement) or sealed in capillary glass tubes (Vitrocom, Mt. Lks. NJ, USA; 0.40 x 4.0 I.D., for real-time Raman micro-spectroscopy evaluation) and photo-cured using a handheld dental curing light (SmartLite max LED curing light, model: 644050, Dentsply International, Milford, DE, USA). The intensity of light irradiation was adjusted through the distance of light to samples.

### Determine DC using FTIR-ATR and peak fitting methods

Degree of conversion (DC) was evaluated immediately after curing using a Thermo Nicolet Nexus 670 FT-IR spectrometer (Thermo Scientific, Madison, Wisconsin, USA) with a KBr beamsplitter, an MCT/A detector and an attenuated total reflectance (ATR) accessory. The areas of absorption peaks of the vinyl group of TEG-DVBE at  $1629\text{ cm}^{-1}$ , and the methacrylate groups of UDMA at  $1638\text{ cm}^{-1}$  were integrated, and the degree of conversion was calculated using the aromatic group of TEG-DVBE at  $1612\text{ cm}^{-1}$  or the amide group of UDMA at  $1537\text{ cm}^{-1}$  as an internal standard.<sup>60</sup> Peaks were resolved with the assistance of the curve fitting program Fityk (version 0.9.8). In order to correct potential discrepancy, a standard curve was produced by plotting varied resin composition ratio values analysed by NMR spectroscopy against the values obtained through FTIR peak fitting. The phenyl absorbance at  $1612\text{ cm}^{-1}$  was the internal standard for TEG-DVBE homo-polymers. DC was calculated according to the

following equation:  $DC = (A1/A0 - A1'/A0') / (A1/A0) 100\%$ , where  $A1/A0$  and  $A1'/A0'$  stand for the peak-area-ratio of vinyl-of-interest and internal standard before and after polymerization, respectively. The vinyl-of-interest may be vinyl groups from TEG-DVBE, UDMA, or both.

#### Sol-gel experiment

The resin specimens were placed in a stainless steel mold (13 mm in diameter and 1 mm in thickness) and then cured for different time scales (10 s, 20 s and 60 s) with a Triad 2000 visible light curing unit (Dentsply, York, PA, USA) fitted with a tungsten halogen light bulb (75 W and 120 V, 43 mW/cm<sup>2</sup>). The samples were then weighed and their DCs were determined by FITR-ATR immediately after the curing. In a pre-weighed vial, each sample was extracted twice using 5 mL deuterated methylene chloride (CDCl<sub>3</sub>) containing 0.01 wt % butylated hydroxytoluene (Aldrich, Saint Louis, MO, USA) via continuous shaking for 48 h. The solution (sol) fractions from these two extractions were combined and concentrated via rotary evaporation under reduced pressure until no further changes in weight were observed. <sup>1</sup>H NMR (Bruker 600 MHz) was conducted for each sol fraction sample to determine the monomer ratio. The remaining gel fraction was collected and dried via in-house vacuum to yield a constant weight, and the DC was measured by FTIR-ATR.

#### Real-time Raman micro-spectroscopy: method description and peak fitting method

Raman spectra were acquired from the dried residues using a Renishaw S1000 micro-Raman spectrometer (Renishaw, Gloucestershire, UK) consisting of a Leica DMLM microscope coupled to a 250 mm focal length imaging spectrograph with a proprietary deep depletion, thermoelectrically cooled (-70 °C) charge-coupled device. For this work, a 632.8 nm helium-neon laser (Model 1144P, JDS Uniphase, Milpitas, CA), holographically ruled 1800 grooves mm<sup>-1</sup> grating, and 20X objective (Leica N PLAN) were used. The excitation laser was focused to a line approximately 50 μm long at the sample position and aligned to the spectrograph entrance slit to maximize throughput. The line focus was utilized to reduce laser power density at the sample. Laser power measured at the sample position was approximately 12 mW. Depending on the desired spectral range, data was acquired using a static grating position covering the Raman shift range from 1275 cm<sup>-1</sup> to 1790 cm<sup>-1</sup> (577 data points) or a grating step scan mode covering the Raman shift range from 500 cm<sup>-1</sup> to 1800 cm<sup>-1</sup> (1369 data points). Integrations time was typically 1 s/pixel. Spectral resolution was approximately 3 cm<sup>-1</sup>. To further minimize any unintended impacts of laser illumination on the photo-polymerization the samples used in the kinetic studies were slowly translated laterally throughout data acquisition. This was done using the motorized microscope translation stage and Raman mapping capabilities in the spectrometer control software (WiRE 3.1, Renishaw, Gloucestershire, UK). Estimation of the degree of conversion of the monomers was accomplished using a direct classical least squares (CLS) multivariate regression approach.<sup>44, 45</sup> Pure spectra of each

monomer were acquired by placing the neat materials in the same vessels as used for the photo-polymerization kinetic studies and collecting spectra with equivalent excitation laser power and integration time to provide spectra that were quantitative relative to one another. The spectral range was restricted to a narrow spectral range from 1625 cm<sup>-1</sup> to 1660 cm<sup>-1</sup>, which corresponds to the stretching modes of the terminal vinyl groups on each monomer. This narrow range was necessary because of band intensity changes and small band shifts observed for many of the vibrational modes as a consequence of the polymerization (see Fig. S2, panel A). Blending of the monomers appeared to introduce small peak shifts ( $\leq 0.5$  cm<sup>-1</sup>) in the vinyl stretching modes that were correlated with the mixture composition. The pure spectra were shifted slightly prior to application of the CLS method in order to minimize the fit residuals. In addition to the two monomer pure spectra, a constant offset was fit in the CLS model in order to correct for baseline variations that arose during the experiments. A simple constant was deemed adequate because the CLS models were fit over a very narrow region of 35 cm<sup>-1</sup>, which corresponds to a spectral band of only 1.75 nm, and fluorescent background interferences generally have much broader spectral profiles. The CLS scores are the contribution of each component of a linear combination of the pure spectrum in a least squares fit of the sample spectra. This is essentially a rigid peak fitting using an arbitrary experimentally measured peak function with a single parameter that corresponds to intensity. The pure spectra were acquired under identical instrumental conditions. Multiple analytical methods (FTIR, Raman and NMR) and different experimental approaches (end-points, sol-gel, and real-time) were applied to determine the composition of copolymers. The results from all of the methods and experimental approaches agreed well with each other. We thus assume that the CLS scores were corresponded directly to the relative composition of monomer mixtures before and during the polymerization. We expect that the decrease in the normalized CLS scores (directly related to peak area) represent a relatively accurate measure of monomer consumption during the polymerization process and the residual terminal unreacted vinyl groups on the monomers once the polymerization has completed. There are potential thermal effects during polymerization and matrix effects in the polymer that may impact the quantitative relationship of these bands relative to the un-polymerized monomer mixture. These could result in errors in DC determinations using these bands that are difficult to predict or correct. While other bands were clearly affected as the polymerization progressed the bands from the unreacted terminal vinyl groups that we were monitoring were not noticeably impacted. No evidence of band broadening or shifting in these bands during polymerization or after. The intensities of these bands still may be impacted but we expect it to be small. The effect is unknown at the present. To estimate the trend of DC of each monomer, the CLS scores for each polymerization data set were normalized by the average score for the given

component from an initial data set (typically ten or more spectra) acquired prior to photo initiation.

The remaining panels of **Fig. S2** show the results from the CLS analysis for an example data set corresponding to one of the equimolar UDMA/TEG-DVBE polymerizations. Panel B is an example fit of the two pure monomer spectra to a sample spectrum. Panel C shows Raman spectral data from a complete polymerization run (truncated to the wavenumber range used for CLS modelling) and the residuals after CLS fitting. Finally, panel D shows the normalized CLS score profiles for the two components over the course of the experiment. The significant difference in signal-to-noise ratio between the two profiles arises from the fact that the Raman cross section of the vinyl stretching mode of TEG-DVBE is approximately an order of magnitude larger than UDMA, which is also evident in the fit in Panel B.

#### Determine monomer reactivity using the NLLS optimization

The composition of copolymers at DC between 1 % and 3 % was determined by real-time Raman micro-spectroscopy and NMR with sol-gel experiment. Seven feed compositions were evaluated. Triplicate measurements were taken at each feed composition. The reactivity ratios from the Mayo-Lewis equation are optimized against this data with the nlinfit function of MATLAB using default parameters and an initial guess of  $r_{\text{TEG-DVBE}} = r_{\text{UDMA}} = 0.5$ . The results of the optimization were used as input into the MATLAB functions nlparci and nlpredci to calculate the reported parameter and model 95% confidence intervals. The sum of squared residuals (SSR) was calculated for a grid (step size .002) of reactivity ratios near the fit solution. An F test was applied to each point of the grid. Any point passing the test:

$$SSR \leq \widehat{SSR} \left( 1 + \frac{p}{n-p} F_{\alpha,p,n-p} \right)$$

was kept as part of the set of points defining the 95% confidence region. In this equation,  $\widehat{SSR}$  is the SSR at the optimal model solution,  $p$  is the number of free parameters (in this work,  $p = 2$ ), and  $n$  is the number of observations used in the optimization. The joint confidence interval was calculated by determining the convex hull of the confidence region using MATLAB's convhull function.

#### Conclusions

In summary, we demonstrated two unique features found in our model monomers, TEG-DVBE and UDMA, and developed analytical tools to identify and evaluate them. First is the synergetic effects of copolymerization on enhancing polymerization rate of the styrene-derivative monomer in a solvent-free environment. It reached 90 % of DC within seconds of visible-light irradiation when copolymerized with UDMA. Second is the azeotropic composition of the copolymer at the equimolar feed. The 1:1 ratio of the feed monomers was maintained in copolymers regardless of the polymerization rate and DC. The azeotropic composition is governed by the monomer chemistry and their interaction with the initiators,

which exceed the influence of diverse monomer viscosity. We also established analytical tools to evaluate the chemical structure and study copolymerization kinetics in real-time. These features and tools enable large-scale production of biocompatible and functional materials with composition-controlled polymeric network, and open new opportunities in material design and development. They will have broad applications in medical devices, packaging, adhesives, automobiles, and 3D printing.

#### Acknowledgements

This work was funded by the National Institute of Dental and Craniofacial Research (U01DE023752). Financial support was also provided through the ADA Foundation. The authors would like to thank Drs. Rafael Bowen, Drago Skrtic and Joseph Antonucci for their technical recommendations. We also would like to thank the Center for Nanoscale Science and Technology (CNST) at NIST for their technical support.

#### Notes and references

- J. C. Barnes, D. J. C. Ehrlich, A. X. Gao, F. A. Leibfarth, Y. V. Jiang, E. Zhou, T. F. Jamison and J. A. Johnson, *Nat. Chem.*, 2015, **7**, 810-815.
- W. Chen and G. B. Schuster, *J. Am. Chem. Soc.*, 2013, **135**, 4438-4449.
- I. Coluzza, P. D. J. van Oostrum, B. Capone, E. Reimhult and C. Dellago, *Phys. Rev. Lett.*, 2013, **110**, 5.
- B. Ghosh and M. W. Urban, *Science*, 2009, **323**, 1458-1460.
- J. W. Kramer, D. S. Treitler, E. W. Dunn, P. M. Castro, T. Roisnel, C. M. Thomas and G. W. Coates, *J. Am. Chem. Soc.*, 2009, **131**, 16042-16044.
- S. C. Solleder and M. A. R. Meier, *Angew. Chem., Int. Ed.*, 2014, **53**, 711-714.
- S. R. White, N. R. Sottos, P. H. Geubelle, J. S. Moore, M. R. Kessler, S. R. Sriram, E. N. Brown and S. Viswanathan, *Nature*, 2001, **409**, 794-797.
- A. Anastasaki, V. Nikolaou, G. S. Pappas, Q. Zhang, C. Wan, P. Wilson, T. P. Davis, M. R. Whittaker and D. M. Haddleton, *Chem. Sci.*, 2014, **5**, 3536-3542.
- N. Baradel, S. Fort, S. Halila, N. Badi and J. F. Lutz, *Angew. Chem., Int. Ed.*, 2013, **52**, 2335-2339.
- W. A. Braunecker and K. Matyjaszewski, *Prog. Polym. Sci.*, 2007, **32**, 93-146.
- C. J. Hawker and K. L. Wooley, *Science*, 2005, **309**, 1200-1205.
- J. F. Lutz, M. Ouchi, D. R. Liu and M. Sawamoto, *Science*, 2013, **341**, 628-636.
- J. T. Xu, K. Jung, A. Atme, S. Shanmugam and C. Boyer, *J. Am. Chem. Soc.*, 2014, **136**, 5508-5519.
- G. Gody, T. Maschmeyer, P. B. Zetterlund and S. Perrier, *Nat. Commun.*, 2013, **4**, 1-9.
- W. R. Gutekunst and C. J. Hawker, *J. Am. Chem. Soc.*, 2015, **137**, 8038-8041.
- F. A. Leibfarth, J. A. Johnson and T. F. Jamison, *Proc. Natl. Acad. Sci. U. S. A.*, 2015, **112**, 10617-10622.
- K. Nakatani, Y. Ogura, Y. Koda, T. Terashima and M. Sawamoto, *J. Am. Chem. Soc.*, 2012, **134**, 4373-4383.
- Z. Zhang, Y. Z. You, D. C. Wu and C. Y. Hong, *Macromolecules*, 2015, **48**, 3414-3421.
- D. L. Patton, K. A. Page, E. A. Hoff, M. J. Fasolka and K. L. Beers, *Polym. Chem.*, 2012, **3**, 1174-1181.

- 20 S. Srichan, N. Kayunkid, L. Oswald, B. Lotz and J. F. Lutz, *Macromolecules*, 2014, **47**, 1570-1577.
- 21 R. X. E. Willemse and A. M. van Herk, *J. Am. Chem. Soc.*, 2006, **128**, 4471-4480.
- 22 E. Andrzejewska, *Prog. Polym. Sci.*, 2001, **26**, 605-665.
- 23 K. S. Anseth, C. M. Wang and C. N. Bowman, *Macromolecules*, 1994, **27**, 650-655.
- 24 W. D. Cook, *Polymer*, 1992, **33**, 600-609.
- 25 M. L. Coote, L. P. M. Johnston and T. P. Davis, *Macromolecules*, 1997, **30**, 8191-8204.
- 26 R. K. Roy and J. F. Lutz, *J. Am. Chem. Soc.*, 2014, **136**, 12888-12891.
- 27 X. C. Pan, M. Lamson, J. J. Yan and K. Matyjaszewski, *ACS Macro Lett.*, 2015, **4**, 192-196.
- 28 B. P. Fors and C. J. Hawker, *Angew. Chem., Int. Ed.*, 2012, **51**, 8850-8853.
- 29 J. Xuan and W. J. Xiao, *Angew. Chem., Int. Ed.*, 2012, **51**, 6828-6838.
- 30 J. M. R. Narayanam and C. R. J. Stephenson, *Chem. Soc. Rev.*, 2011, **40**, 102-113.
- 31 T. P. Yoon, M. A. Ischay and J. N. Du, *Nat. Chem.*, 2010, **2**, 527-532.
- 32 J. L. Ferracane, *Dent. Mater.*, 2011, **27**, 29-38.
- 33 G. Huyang, A. E. Debertin and J. Sun, *Mater. Des.*, 2016, **94**, 295-302.
- 34 H. Lin, D. N. Zhang, P. G. Alexander, G. Yang, J. Tan, A. W. M. Cheng and R. S. Tuan, *Biomaterials*, 2013, **34**, 331-339.
- 35 F. P. W. Melchels, J. Feijen and D. W. Grijpma, *Biomaterials*, 2010, **31**, 6121-6130.
- 36 J. R. Tumbleston, D. Shirvanyants, N. Ermoshkin, R. Januszewicz, A. R. Johnson, D. Kelly, K. Chen, R. Pinschmidt, J. P. Rolland, A. Ermoshkin, E. T. Samulski and J. M. DeSimone, *Science*, 2015, **347**, 1349-1352.
- 37 A. Gonzalez-Bonet, G. Kaufman, Y. Yang, C. Wong, A. Jackson, G. Huyang, R. Bowen and J. Sun, *Biomacromolecules*, 2015, **16**, 3381-3388.
- 38 C. J. E. Floyd and S. H. Dickens, *Dent. Mater.*, 2006, **22**, 1143-1149.
- 39 A. E. Papanikolaou, T. Eliades, F. Cellesi, D. C. Watts and N. Silikas, *Dent. Mater.*, 2013, **29**, 898-905.
- 40 I. Sideridou, V. Tserki and G. Papanastasiou, *Biomaterials*, 2002, **23**, 1819-1829.
- 41 N. C. Maiti, M. M. Apetri, M. G. Zagorski, P. R. Carey and V. E. Anderson, *J. Am. Chem. Soc.*, 2004, **126**, 2399-2408.
- 42 P. Spencer, Y. Wang, M. P. Walker, D. M. Wieliczka and J. R. Swafford, *Journal of Dental Research*, 2000, **79**, 1458-1463.
- 43 J. W. Stansbury and S. H. Dickens, *Dent. Mater.*, 2001, **17**, 71-79.
- 44 H. Martens and T. Naes, *Multivariate Calibration*, Wiley, 1992.
- 45 M. K. Antoon, J. H. Koenig and J. L. Koenig, *Appl. Spectrosc.*, 1977, **31**, 518-524.
- 46 L. Rey, J. Galy and H. Sautereau, *Macromolecules*, 2000, **33**, 6780-6786.
- 47 T. F. Scott, W. D. Cook, J. S. Forsythe, C. N. Bowman and K. A. Berchtold, *Macromolecules*, 2003, **36**, 6066-6074.
- 48 P. J. Flory, *Principles of polymer chemistry*, Cornell University Press, 1983.
- 49 G. Odian, *Principles of polymerization*, Wiley, 2004.
- 50 J. W. Stansbury and S. H. Dickens, *Polymer*, 2001, **42**, 6363-6369.
- 51 F. R. Mayo and F. M. Lewis, *J. Am. Chem. Soc.*, 1944, **66**, 1594-1601.
- 52 D. L. Patton, K. A. Page, C. Xu, K. L. Genson, M. J. Fasolka and K. L. Beers, *Macromolecules*, 2007, **40**, 6017-6020.
- 53 A. M. vanHerk and T. Droge, *Macromol. Theory Simul.*, 1997, **6**, 1263-1276.
- 54 O. F. Olaj, I. Schnollbitai and P. Kremminger, *Eur. Polym. J.*, 1989, **25**, 535-541.
- 55 S. Asmusen, G. Arenas, W. D. Cook and C. Vallo, *Dent. Mater.*, 2009, **25**, 1603-1611.
- 56 S. Asmussen, G. Arenas, W. D. Cook and C. Vallo, *Eur. Polym. J.*, 2009, **45**, 515-522.
- 57 W. F. Schroeder, M. I. Aranguren and J. Borrajo, *J. Appl. Polym. Sci.*, 2010, **115**, 3081-3091.
- 58 J. G. Leprince, W. M. Palin, M. A. Hadis, J. Devaux and G. Leloup, *Dent. Mater.*, 2013, **29**, 139-156.
- 59 M. G. Neumann, C. C. Schmitt, G. C. Ferreira and I. C. Correa, *Dent. Mater.*, 2006, **22**, 576-584.
- 60 R. M. Guerra, I. Duran and P. Ortiz, *J. Oral Rehabil.*, 1996, **23**, 632-637.

## Graphical Abstract

This work introduces a cross-linked resin network with controlled chemical composition, a clinically practical procedure to make it *in situ*, and appropriate analytical tools for chemical structure and kinetic studies.

